Deep eutectic solvent mixed ionic liquids achieve highly unified wave absorption and mechanical properties

Yuntong Wang[1)], Tao Zhang[1)], Shengchong Hui[1)], Zijing Li[1)], Geng Chen[1)], Limin Zhang[1,2)] *, Hongjing Wu[1)], *

[1)] MOE Key Laboratory of Material Physics and Chemistry under Extraordinary, School of Physical Science and Technology, Northwestern Polytechnical University, Xi'an 710072, China

[2)] Research & Development Institute of Northwestern Polytechnical University in Shenzhen, Sanhang Science &Technology Buliding, No. 45th, Gaoxin South 9th Road, Nanshan District, Shenzhen City, 518063, China

* Corresponding authors.

E-mail address: liminzhang@nwpu.edu.cn (L. Zhang), wuhongjing@nwpu.edu.cn (Hongjing Wu).

Supplementary Figures

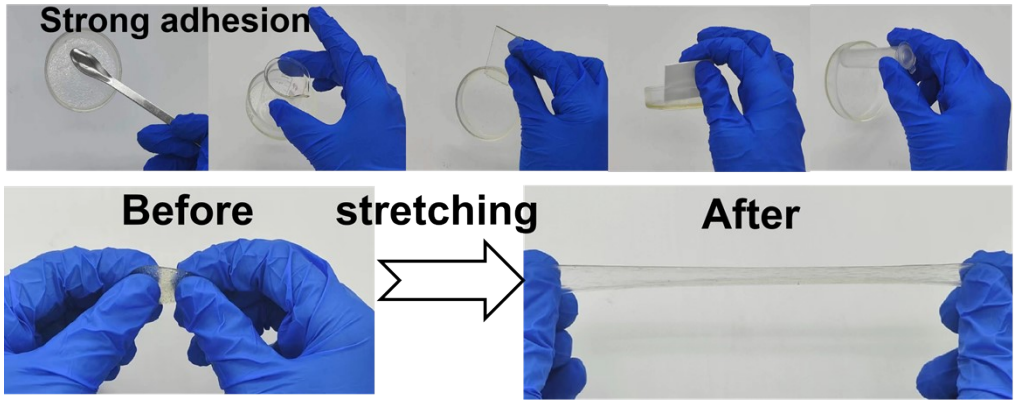

Fig. S1. Strong adhesion and stretching of deep eutectic ionogels.

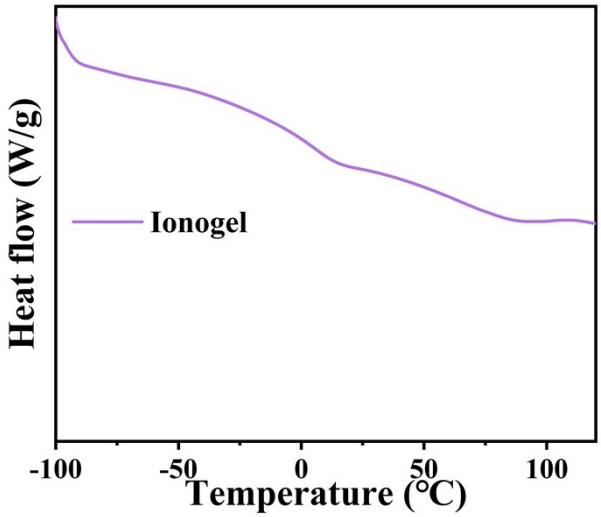

Fig. S2. The DSC curve of Ionogel, show no glass transition temperature. The presence of EMIES, with a low glass transition temperature (−78.4 °C), in the Ionogel, along with the hydrophilic nature of EMIES and DMA, leads to the incorporation of a small amount of water, which enhances intermolecular interactions through hydrogen bonding, thereby reducing the mobility and freedom of the molecules and lowering the glass transition temperature. The clusters formed by water and EMIES further decrease the transition temperature. Additionally, the electrostatic attraction between the positively charged main chain and $TFSI^-$ and ES^- anion increases the degree of dissociation of the ions, thereby lowering the transition temperature. As a result, no glass transition temperature is observed in the DSC curve of the Ionogel

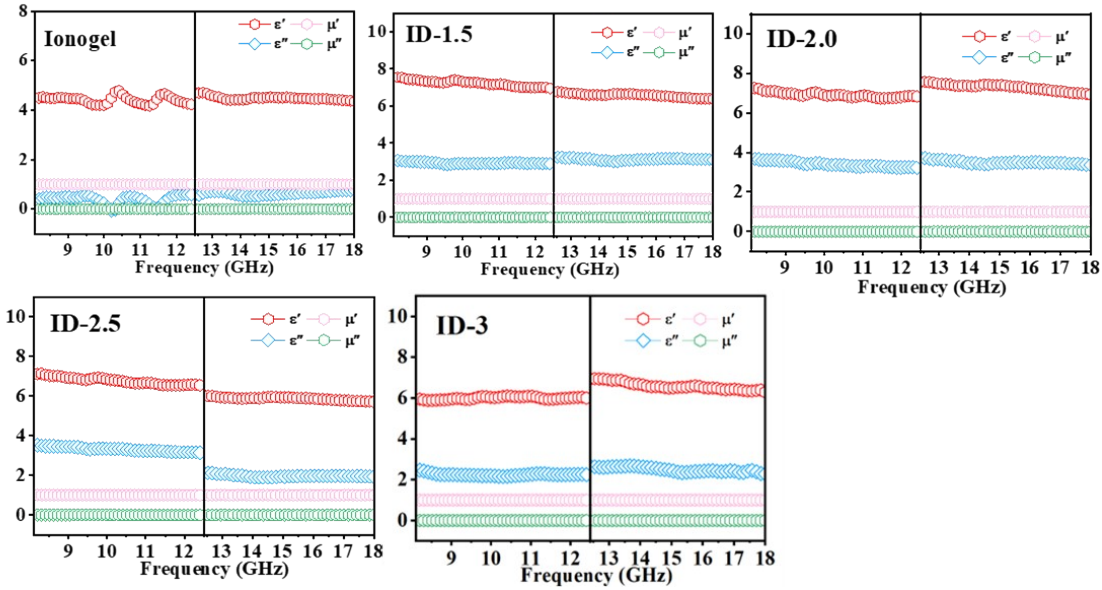

Fig. S3. permittivity of deep eutectic ionic gels

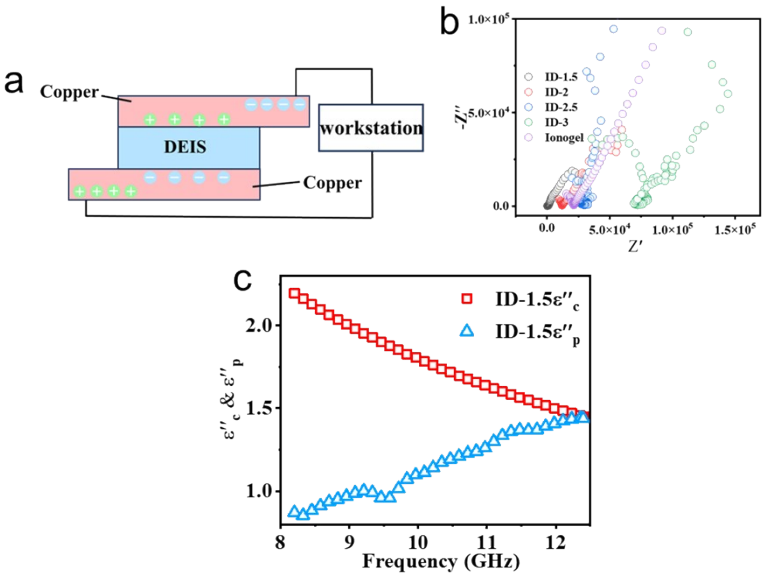

Fig. S4. a. Schematic diagram of electrochemical workstation. b. Electrochemical impedance plots of deep eutectic ionic gels. c. ε''_c and ε''_p of ID-1.5.

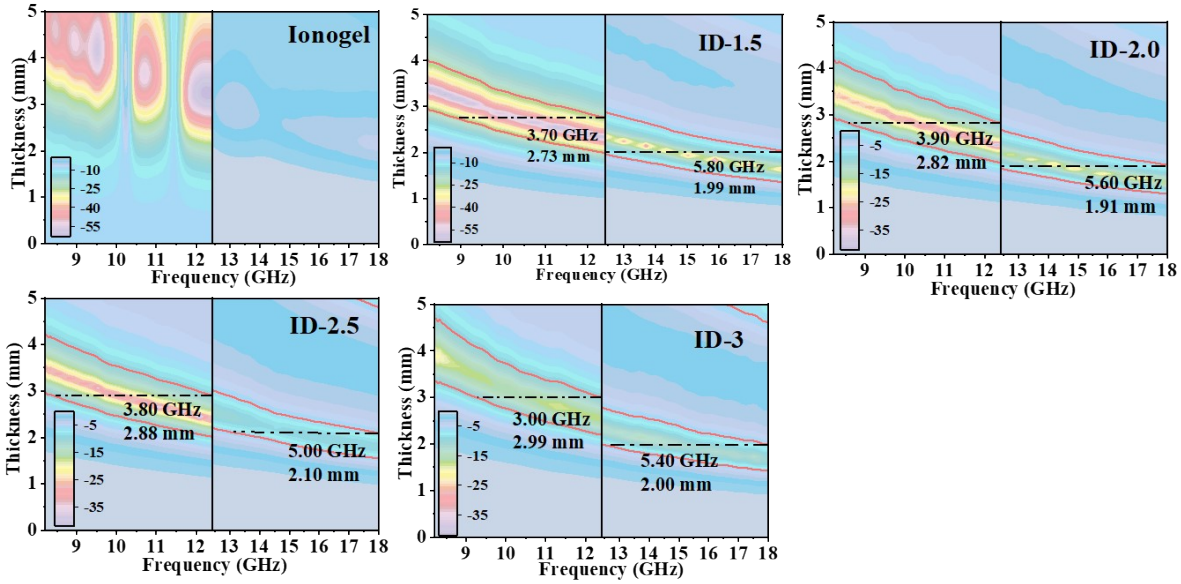

Fig. S5. Electromagnetic wave absorption properties of deep eutectic ionic gels at 8-18 GHz.

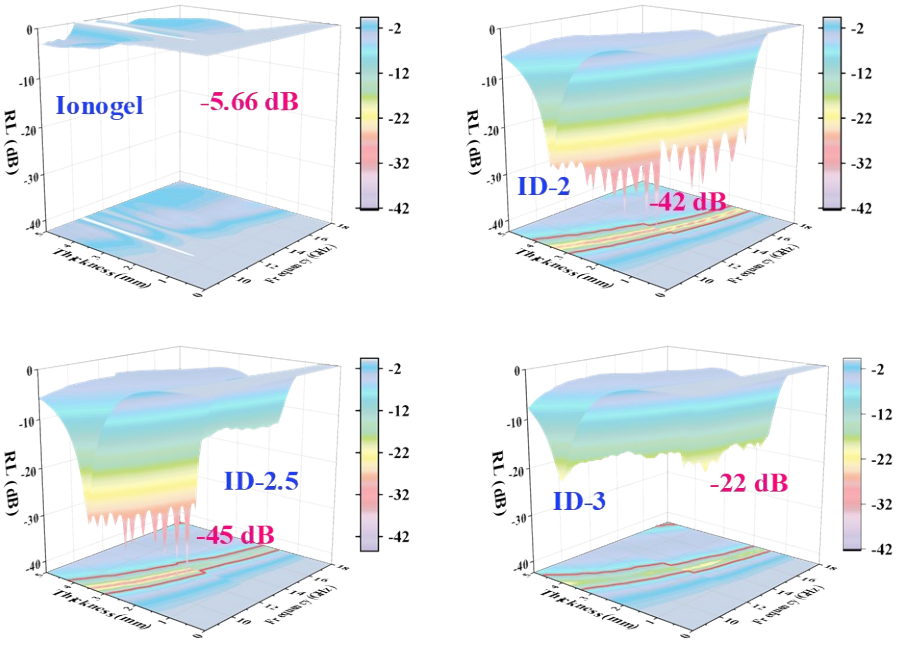

Fig. S6. Reflection loss intensity values for deep eutectic ionic gels.

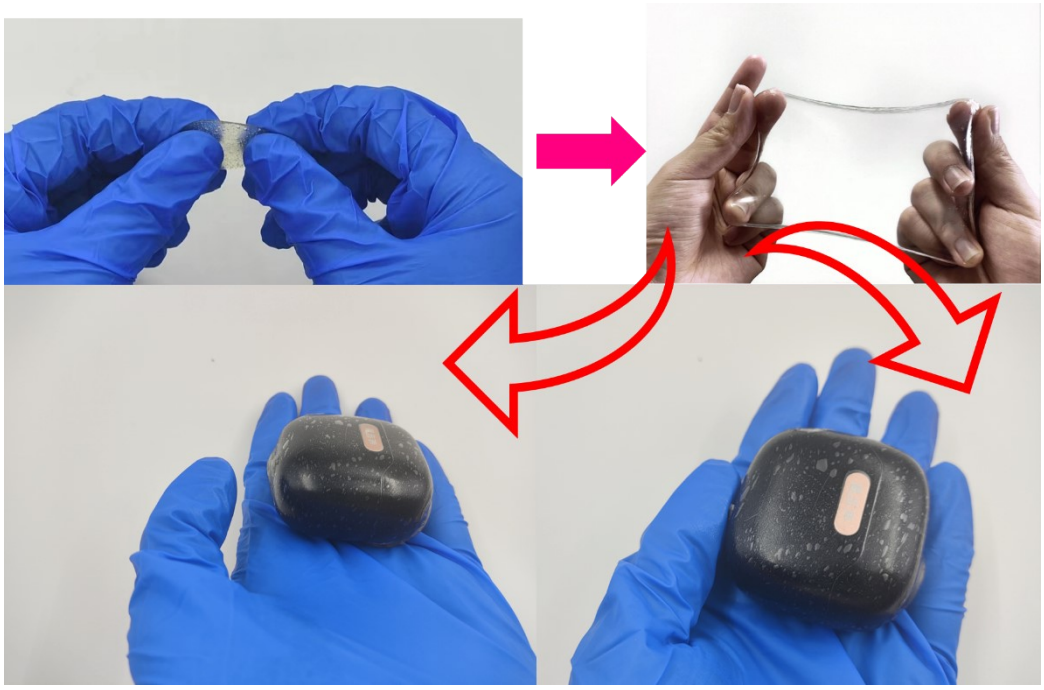

Fig. S7. Tensile ductility and encapsulation of deep eutectic ionic gels

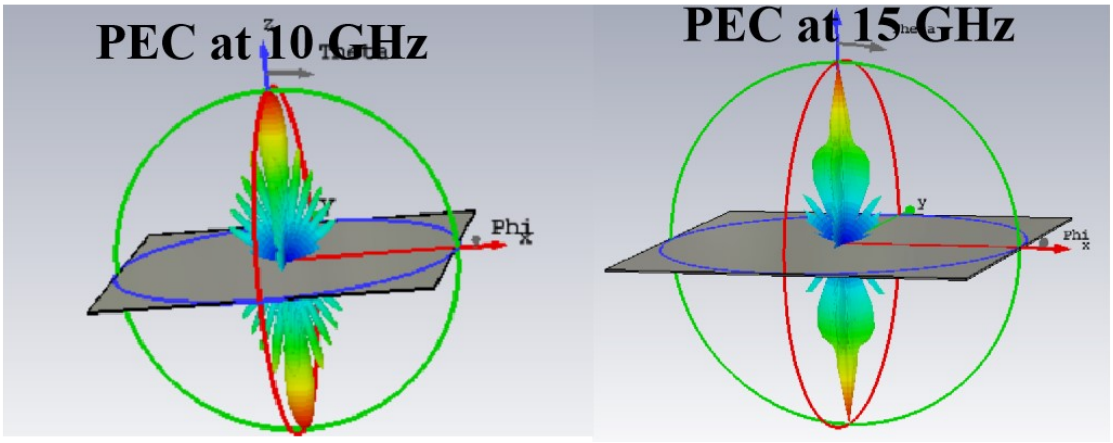

Fig. S8. Radar signals received by PEC's RCS value

Fig. S9. Testing the tensile properties of deep eutectic ionic gels using an electronic universal tensile machine.

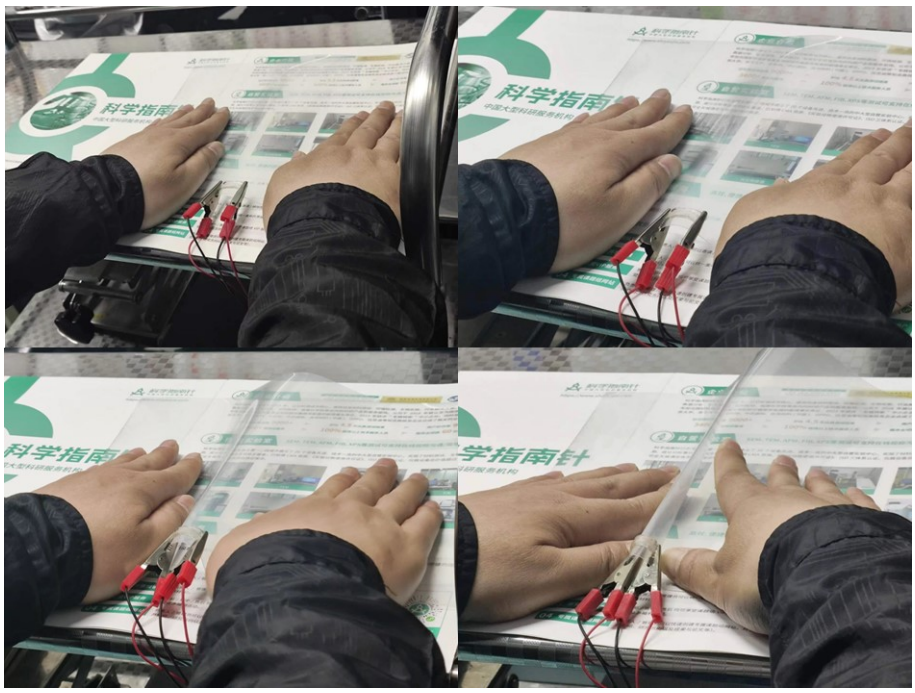

Fig. S10. Strain Sensing Performance Tests for DEIs

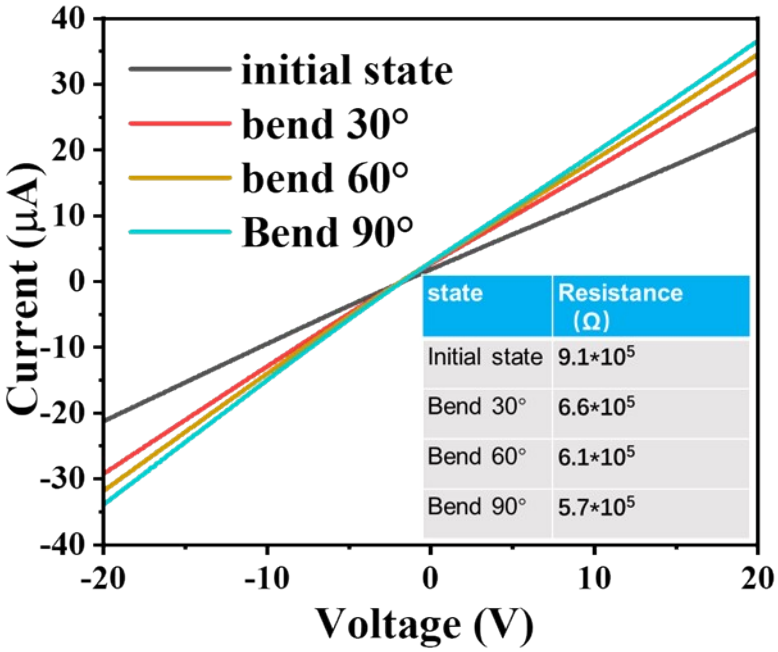

Fig. S11. Voltage-current curves with bending angle.